MICROVASCULAR RESEARCH 51, 39–50 (1996)
Article No. 0005

Reconsidering the Effect of Local Plasma Convection in a Classical Model of Oxygen Transport in Capillaries

CEES BOS,*,[1] LOUIS HOOFD,* AND THOM OOSTENDORP†

*Department of Physiology, University of Nijmegen, P.O. Box 9101, 6500 HB Nijmegen, The Netherlands; and †Department of Medical Physics and Biophysics, University of Nijmegen, P.O. Box 9101, 6500 HB Nijmegen, The Netherlands

Received December 5, 1994

In 1970, Aroesty and Gross investigated the influence of local plasma convection in between two successive red blood cells (RBC) in a capillary on the local oxygen transfer into tissue by combining convectional and diffusional oxygen transport. They concluded that the effect of local plasma convection on oxygen transport in the capillaries was insignificant. Here it is shown that this result was due to their choice of flat oxygen concentration profiles as boundary conditions. In fact, the plasma motion can be of importance when more realistic oxygen concentrations are used as boundary conditions. The fluxes of oxygen through the capillary wall could be up to 50% larger as compared to those of Aroesty and Gross, especially for low hematocrit values and for maximally working muscle. Since the boundary concentrations in the model of the current paper are fixed, chosen not to be influenced by the transport processes, calculations will not show to what extent motion really enhances the oxygen transport, and should be considered as rough indications of the effect of plasma motion. The results in this investigation indicate that in capillaries motion has to be taken into account under conditions of low hematocrit or high RBC velocity.

INTRODUCTION

In the microcirculation, both diffusion and convection play an important role in oxygen transport to tissue. Of these two transport phenomena, the former is the better defined and relatively easy to incorporate in mathematical models of tissue oxygenation. It was the first to be modelled (Krogh, 1919). The latter is more complicated and in most models only partly implemented. In these models, only the global transport of blood, including red blood cells (RBC), is taken into account. In this type of 'global' convection, radial components of the velocity of the plasma are neglected. A large number of authors investigated tissue oxygenation by means of diffusion and global convection (e.g., Groebe, 1990; Tsai and Intaglietta, 1993; Secomb *et al.*, 1993; Sharan *et al.*, 1991). A major difference among these models is how the oxygen transport phenomena in the capillaries are described. There is more to be said about convection in the capillaries.

In small capillaries the RBCs fill the capillary completely or at least almost com-

[1] To whom correspondence and reprint requests should be addressed. Fax: +31 24-3540535. E-Mail: C.Bos@fysio.kun.nl.

0026-2862/96 $12.00

pletely in the transverse direction. Between the RBCs there will be gaps of various lengths filled with plasma. In these gaps local convection may induce motion of the plasma, which might enhance the oxygen transport into the tissue. This can be investigated by coupling the local convection to the diffusion by use of the plasma velocity components in the mass-balance equations. For this purpose, a model of the local convection is needed.

Convection was extensively investigated for relatively simple geometries in the sixties and reviews of these studies can be found in literature (Gross and Aroesty, 1972; Huang, 1971; Leonard and Jørgensen, 1974). Both (semi-) analytical (Duda and Vrentas, 1971; Lew and Fung, 1969; Wang and Skalak, 1969) and numerical solutions (Aroesty and Gross, 1970; Bugliarello and Hsiao, 1970) are to be found. An analogue of oxygen diffusion is heat transfer. The effect of motion on heat transport was investigated experimentally by, for instance, Prothero and Burton (1961). They found motion could improve heat transfer by up to twofold. However, Aroesty and Gross (1970) showed that one has to be careful in extrapolating these results to oxygen transport. Therefore they developed a mathematical model which combined local convection and diffusion. They concluded from this model that the effect of plasma motion on local oxygen transport was insignificant. Their study was the basic justification for omitting local plasma convection in investigations of oxygen transport in capillaries.

When one carefully looks at the concentration gradients that are calculated with models based on diffusion and net convection, it is obvious that the oxygen concentration profile at the plasma–tissue and the plasma–RBC interface is curved, with a higher value at the upstream RBC and a lower value at the downstream RBC (Groebe and Thews, 1989; Groebe, 1990; Hoofd, 1992). These curved profiles originate from the particulate nature of blood and the difference in concentration at the up- and downstream RBC is caused by the oxygen loss of the RBCs. Aroesty and Gross, however, set the concentration at the plasma–tissue interface and the plasma–RBC interfaces to constant values, with the same value at both RBCs. This discrepancy in concentration at the boundary of the plasma between the model of Aroesty and Gross and the values that are available from current tissue models, will be considered in this paper. If the outcome of the study of Aroesty and Gross does not depend on the choice of boundary concentrations, their conclusion will be generally applicable. In other words, if local plasma convection never affects oxygen transfer, this should be true for every type of boundary condition.

In this study more realistic boundary conditions are applied to the model of Aroesty and Gross (1970). The results will show whether the influence of plasma motion on local oxygen supply really can be ignored or that further study is needed.

MATHEMATICAL MODEL

The model is developed for a cylindrical plasma gap between two RBCs. Consequently the cylindrical coordinate system $\bar{r} = (r, \phi, z)$ is used. Because of axial symmetry there is no dependence on the azimuthal angle ϕ, consistent with the layout of the model of Aroesty and Gross. In Fig. 1 it is indicated that half the distance between the RBCs is L, the radius of the capillary is R and the velocity of the RBCs is v_{RBC}. Since only the effect of local convection was investigated the plasma motion

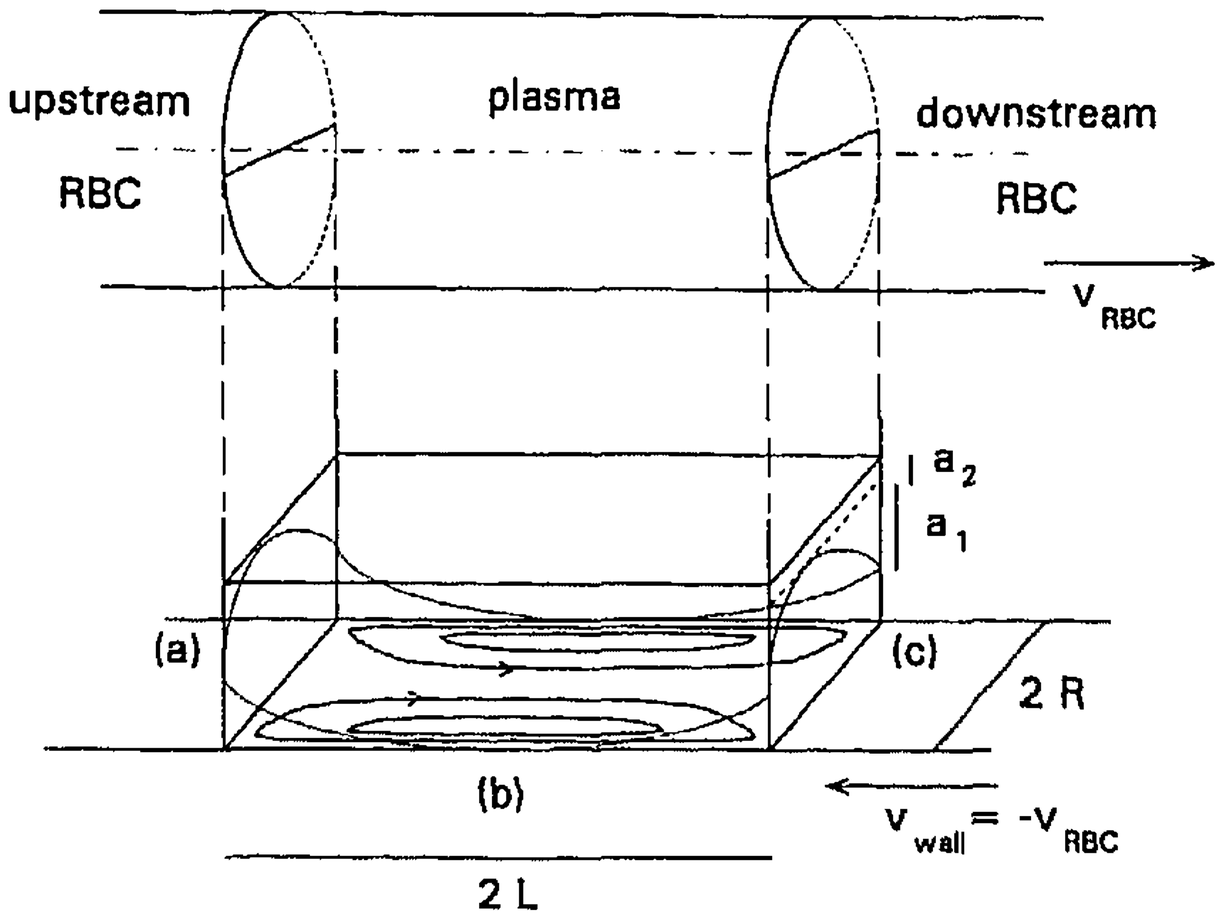

FIG. 1. Lay-out of model (upper part) and boundary concentrations (lower part). A rough depiction of the streamlines is shown for $R/L = 1.0$.

was considered relative to the RBCs, which simplifies the describing equations. This is similar to a moving wall with fixed RBCs where the wall moves with velocity $-v_{RBC}$. The equations are extensively described by Aroesty and Gross (1970). Next the major equations that set up the model will be shown.

The fluid dynamics is modelled by two equations: the equation of continuity, which is the mass balance, and the equation of motion, which is the momentum balance. Unlike blood, plasma is considered to be a Newtonian fluid, i.e., with a constant density ρ and a constant viscosity μ. This leads to the Navier–Stokes equation, but for low Reynolds numbers, with a characteristic distance d ($\mathrm{Re} = \rho \cdot v \cdot d/\mu < 0.1$), the equation can be simplified to Stokes flow (Bird *et al.*, 1960). In capillaries the Reynolds number is approximately 10^{-3}. Thus, the fluid dynamics is described by

$$\begin{cases} (\vec{\nabla} \cdot \vec{v}) = 0 \\ \vec{\nabla} p = \mu \nabla^2 \vec{v}, \end{cases} \tag{1}$$

where p is the pressure, $\vec{v}$ is the velocity of the fluid, the dot denotes the inner product of two vectors, $\vec{\nabla}$ is the gradient operator, and ∇^2 is the Laplace operator. For the chosen coordinate system the gradient and Laplace operator are defined as

$$\vec{\nabla} = \begin{pmatrix} \dfrac{\partial}{\partial r} \\ \dfrac{\partial}{\partial z} \end{pmatrix} \qquad \nabla^2 = \frac{\partial^2}{\partial r^2} + \frac{1}{r}\frac{\partial}{\partial r} + \frac{\partial^2}{\partial z^2}. \tag{2}$$

The equations of motion and continuity are solved by means of the stream function Ψ, where the velocity components are expressed as derivatives of Ψ. For this case the stream function is defined as the solution of

$$u_z = -\frac{1}{r}\frac{\partial \Psi}{\partial r}, \quad u_r = \frac{1}{r}\frac{\partial \Psi}{\partial z}, \tag{3}$$

where u_z and u_r are, respectively, the axial and radial component of the dimensionless velocity $\bar{u}$, where $\bar{u} = \bar{v}/v_{RBC}$. The stream function can either be solved from a fourth order partial differential equation (PDE) or from a system of two second order PDEs. Here, we follow Aroesty and Gross (1970) by solving a system of two equations, since the number of grid points needed in numerical computation is less than with the fourth order equation. To solve the stream function, two simultaneous equations have to be solved:

$$\begin{cases} E^2\Psi = r\zeta \\ E^2(r\zeta) = 0 \end{cases}, \text{ with } \zeta = \frac{\partial u_r}{\partial z} - \frac{\partial u_z}{\partial r} \text{ and } E^2 = \frac{\partial^2}{\partial r^2} - \frac{1}{r}\frac{\partial}{\partial r} + \frac{\partial^2}{\partial z^2}, \tag{4}$$

where ζ is the vorticity, which is the curl of the velocity ($\bar{\nabla} \times \bar{u}$). The boundary condition for the fluid dynamics is zero slip at the boundary surfaces, which leads to stream lines of constant Ψ, similar to those in Fig. 1.

The velocity components derived from the stream function are needed for the mass transfer equation. When steady state is assumed, the mass conservation equation becomes

$$(\bar{v} \cdot \bar{\nabla} c) = D\nabla^2 c, \tag{5}$$

where c is the concentration, and D is the diffusivity. The motion is introduced in the left-hand side and the diffusion is defined in the right-hand side. The equations are made dimensionless by means of the characteristic length L, the characteristic velocity v_{RBC}, and the dimensionless concentration $c^* = (c - c_0)/c_1$, which is calculated from the equation

$$\mathrm{Pe}\left(u_z \frac{\partial c^*}{\partial z} + u_r \frac{\partial c^*}{\partial r}\right) = \frac{\partial^2 c^*}{\partial r^2} + \frac{1}{r}\frac{\partial c^*}{\partial r} + \frac{\partial^2 c^*}{\partial z^2}, \tag{6}$$

where $\mathrm{Pe} = v_{RBC} \cdot L/D$ is the Peclet number. It can easily be seen that Pe is zero if the local convection is neglected. Then, the local mass transfer is entirely based on diffusion.

To calculate the dimensionless concentration profile, boundary conditions for the concentration at the borders of the plasma are needed. Aroesty and Gross used (dimensionless) concentrations of 1 at the tissue–plasma interface and 0 at the RBC–plasma interface, which implies oxygen uptake by the RBCs. Exactly the same effect of plasma motion will be found when the boundary concentrations are set to 0 for the tissue–plasma interface and 1 for the RBC–plasma interface, implying oxygen release from the RBCs. It is obvious that these are unrealistic conditions, resulting in singularities in the describing equations at the corners of the gap. Still, these concentrations are useful indeed as a first investigation of the effect of motion. More realistic boundary concentrations might be obtained from models that rely on diffusion and global convec-

tion, even though these models do not take into account the motion of plasma. The curved concentration profiles as obtained from such models (Bos *et al.*, 1995; Groebe and Thews, 1989; Groebe, 1990; Hoofd, 1992) can be used as boundary concentrations. For simplicity these boundary concentrations will be approximated by second order polynomials. In this study we use the model of Bos *et al.* (1995) to approximate these boundary concentrations. The equations are

$$\begin{cases} c^* = 1 - \dfrac{a_1}{R^2} r^2 & \text{upstream RBC } (z = -L) \\ c^* = 1 - a_2 - \dfrac{a_1}{R^2} r^2 & \text{downstream RBC } (z = L) \\ c^* = \dfrac{a_3}{L^2} z^2 - \dfrac{a_2}{2L} z + a_4 & \text{capillary border } (r = R) \\ a_3 = 1 - a_1 - \dfrac{a_2}{2} - a_4 & \\ a_4 = \dfrac{a_2^2}{16 a_3}, & \end{cases} \tag{7}$$

where a_1 is the concentration drop from the center of the RBC to the border, and a_2 is the concentration drop between two successive RBCs. Note that there is a maximum and a minimum for c^* of 1 and 0, respectively, and that the concentrations are continuous at the edges.

Similar to the convection, the oxygen flux through the capillary wall can also be considered on a local and a global scale. To investigate the effect of motion on the local mass transfer Aroesty and Gross introduced a ratio $\dot{m}$ of gradients at each location along the boundary of the gap, defined as

$$\dot{m} = \frac{\text{Local mass transfer rate (convection + diffusion)}}{\text{Local mass transfer rate (diffusion only)}} . \tag{8}$$

$\dot{m}$ is defined along all boundaries: at the capillary wall $\dot{m} = (\partial c/\partial r)_{Pe}/(\partial c/\partial r)_{Pe=0}$ and along the RBC $\dot{m} = (\partial c/\partial z)_{Pe}/(\partial c/\partial z)_{Pe=0}$. This ratio shows the effect of motion on the local mass transfer. Although this provides interesting information, it does not provide an easy estimate of the change in overall oxygen fluxes through the capillary wall. The change in the local gradient does not necessarily show whether the global flux is changed, since a large change of a small gradient might be compensated for by a small change of a large gradient. Therefore we introduce φ, the ratio of the global flux across the entire boundary with plasma motion to the global flux without motion. The difference in oxygen flux at the capillary wall can be calculated by means of a flux ratio which is defined as:

$$\varphi(\mathrm{Pe}) = \frac{\int_{-L}^{L} J_r dz|_{Pe}}{\int_{-L}^{L} J_r dz|_{Pe=0}} = \frac{\int_{-L}^{L} \left(\dfrac{\partial c}{\partial r}\right) dz|_{Pe}}{\int_{-L}^{L} \left(\dfrac{\partial c}{\partial r}\right) dz|_{Pe=0}} . \tag{9}$$

Essentially, $\dot{m}$ and φ describe the same phenomenon, $\dot{m}$ local and φ global.

The results of model calculations will be presented and compared both for situations as considered by Aroesty and Gross and for more realistic boundary concentrations. Similarities between the two approaches are that calculation of the local convection is identical and that the calculation of the oxygen transfer is based on the use of fixed oxygen concentration profiles as boundary conditions. The difference is the shape of the oxygen profiles that are used as boundary conditions for the calculation of the oxygen concentrations throughout the plasma.

RESULTS

The model was used to perform calculations for rat heart. The diameter of capillaries varies, but since in the present model the RBC fills the capillary, only a small radius is considered. The volume of an RBC is 61 $(\mu m)^3$ (Altman *et al.*, 1958). For $R = L$ and a 40% hematocrit this results in a capillary radius of 2.44 μm, which is a typical value for rat heart capillaries. The diffusion coefficient of oxygen in plasma is about $2 \cdot 10^{-9}$ $m^2 \cdot s^{-1}$ (Groebe, 1990; Nair *et al.*, 1990). Based on a average RBC velocity of 1 $mm \cdot s^{-1}$ (Rakusan and Blahitka, 1974), Hoofd *et al.* (1990) calculated a value for $\alpha F/l$ which leads to $v/D = (\alpha F/l)/(\pi R^2) = 0.565$ $(\mu m)^{-1}$ for "resting" rat heart muscle (i.e., nonexercising rat). These values can be used to calculate the Peclet number, which is indicative of the amount of convection. Therefore, to investigate the effect of motion the equations were solved for different Peclet numbers. The maximal value for Pe is found for a low hematocrit together with a high velocity. Here, the lowest hematocrit is 20% and maximal value for v/D is five times 0.565 $(\mu m)^{-1}$, which results in Pe = 18. This maximal value for v/D is chosen since for different species, the coronary flow can increase about five times for heavy work (Honig, 1981; Lochner, 1971; Van Citters and Franklin, 1969).

In Fig. 2 the calculated oxygen profiles are shown for Pe = 1 and Pe = 10. To show the effect of local plasma convection on the profiles the difference between those two profiles is also depicted. These figures can also be used to get an impression of the concentration profiles that are used as boundary conditions. In Fig. 3 the corresponding local gradients are shown for A, B, C, and D. The RBCs move from left to right.

In Figs. 3A and 3C, the effect of motion on $\dot{m}$ is shown for boundary conditions similar to those used by Aroesty and Gross (1970). They showed only the $\dot{m}$ along the capillary for $R/L = 1.0$, and it is obvious that motion does alter the local mass transfer but the impact is rather small, since the enhancement at the downstream side is almost cancelled by the changes at the upstream side. When the RBC spacing increases to $R/L = 0.2$ the effect of motion is even less important with the boundary conditions of Aroesty and Gross (not shown). It can also be seen that the flux at the upstream RBC increases while the flux at the downstream RBC decreases, so the contribution of the upstream RBC to the tissue oxygenation increases at the expense of the downstream RBC. This raises the question as to whether the effect of motion is more important when both RBCs have different oxygen concentrations.

This question is addressed together with the investigation of the effect of more realistic continuous oxygen profiles as boundary concentrations. In Table 1 the effect of motion on the total oxygen flux at the capillary border is shown through $\varphi(\ )$ with various boundary concentrations. It can easily be seen that the effect of motion is insignificant for the boundary conditions of Aroesty and Gross. When either a

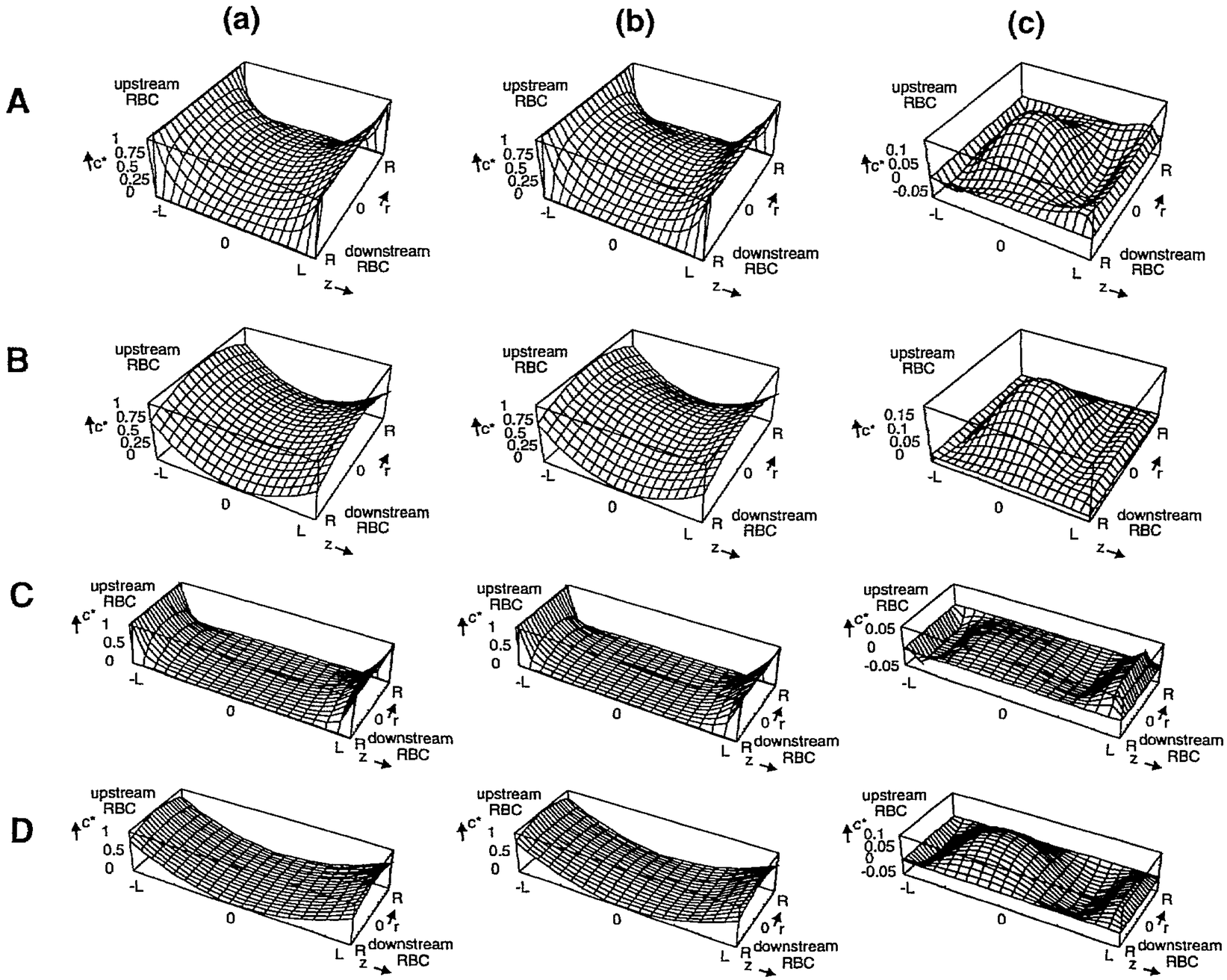

FIG. 2. Oxygen concentration profiles for Pe = 1 (a) and Pe = 10 (b) and concentration difference (c) between Pe = 10 and Pe = 1. A, B, C, and D are for the same hematocrit and boundary conditions as their corresponding examples in Fig. 3 and Table 1. The RBCs move from left to right.

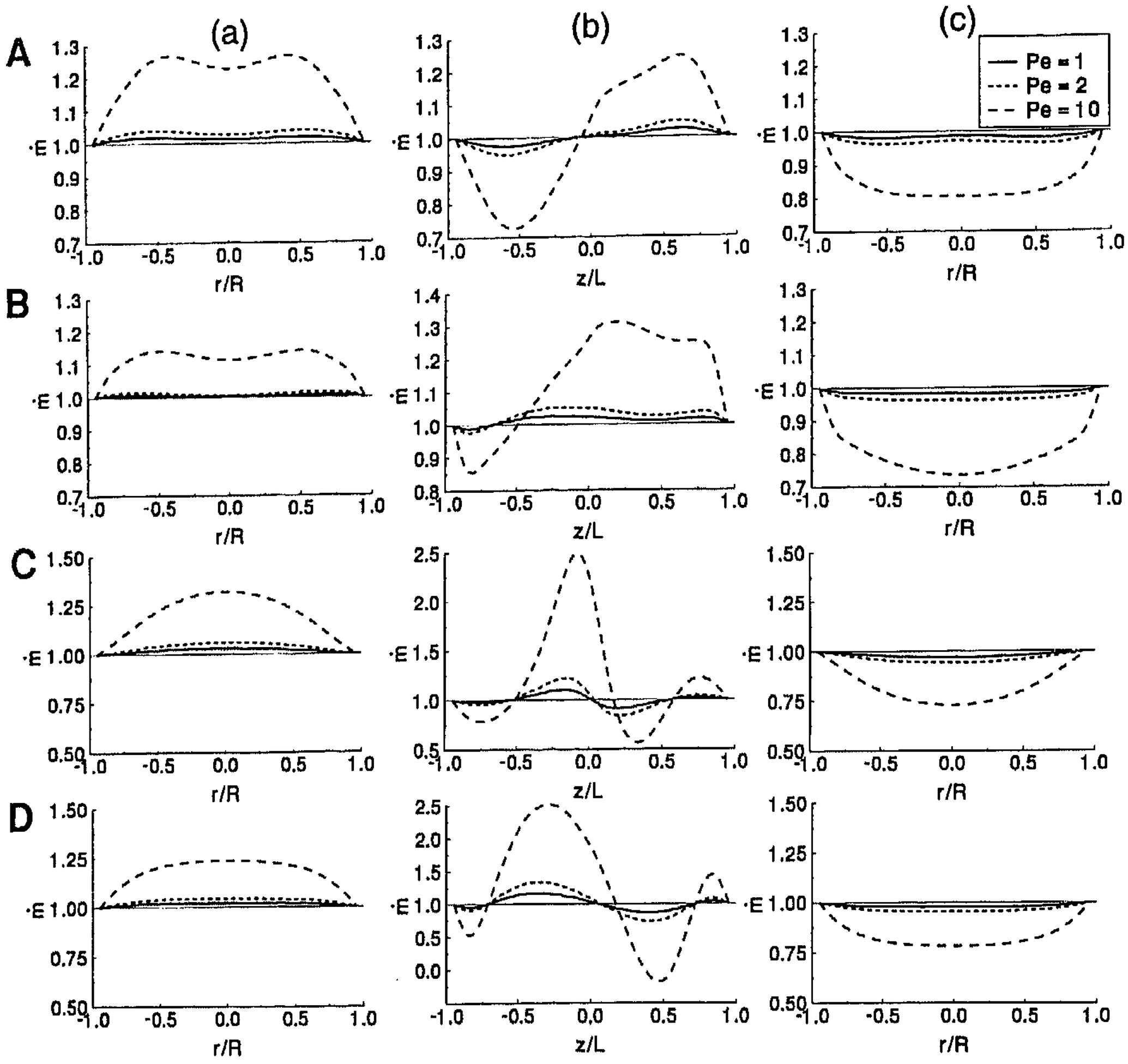

FIG. 3. Local mass transfer ratio at the gap borders: upstream (a), tissue (b), and downstream (c). The boundary concentrations are identical to those in Fig. 2 and in Table 1.

concentration drop between two successive RBCs or curved boundary concentrations are introduced separately (not shown here) the effect of motion becomes visible. In Table 1 a combination of both the concentration drop and the curved profile is used

TABLE 1
Effect of Motion on the Flux at the Capillary Wall

Fig. 2	Hct	a_1	a_2	R/L	Pe (Rest)	Pe (Max)	$\varphi(1)$	$\varphi(2)$	$\varphi(10)$	φ(Pe) (Rest)	φ(Pe) (Max)
A	40%	0	0	1.0	1.4	6.8	1.00	1.00	1.00	1.00	1.00
B	40%	0.34	0.18	1.0	1.4	6.8	1.01	1.03	1.15	1.02	1.10
C	20%	0	0	0.4	3.7	18	1.00	1.00	1.00	1.00	1.00
D	20%	0.23	0.12	0.4	3.7	18	1.01	1.02	1.24	1.07	1.51

Note. a_1 and a_2 from equation (7), and $\varphi(\ )$ from equation (9). Rows with $a_1 = a_2 = 0$ are boundary concentrations as used by Aroesty and Gross (1970), and in the remaining rows a_1 and a_2 are estimated from Bos *et al.* (1995).

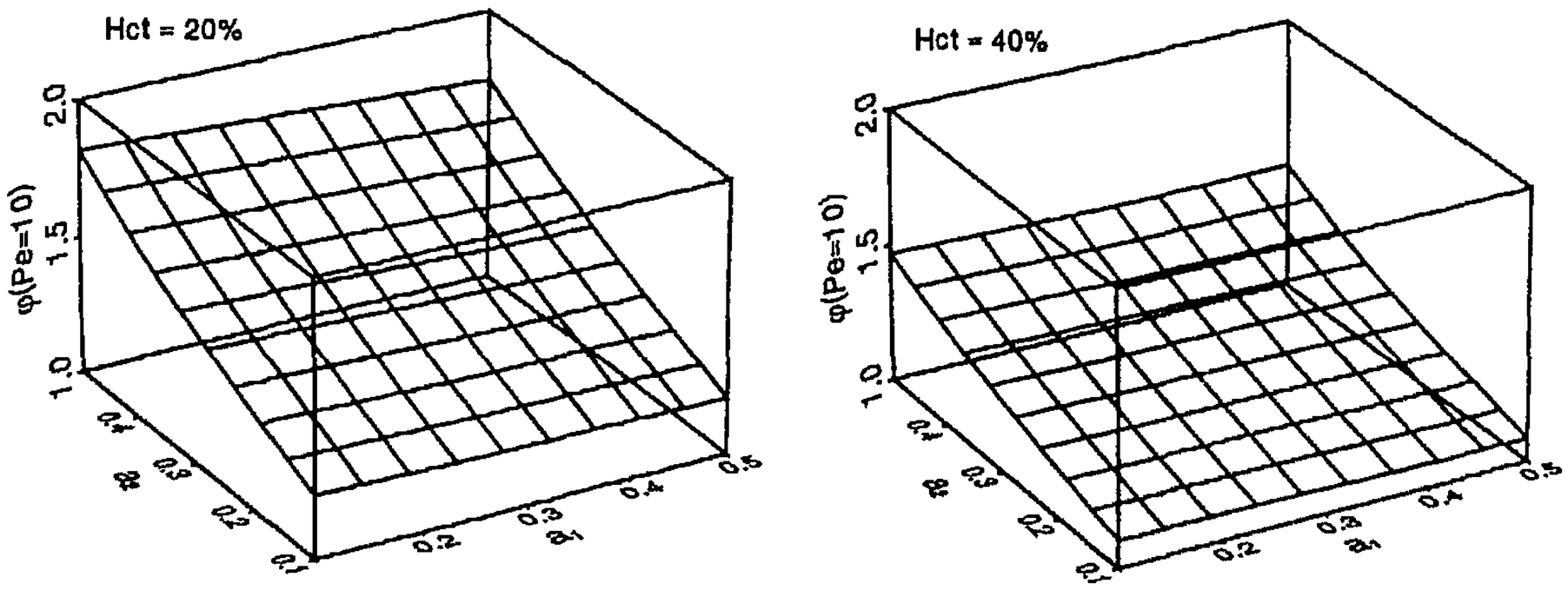

FIG. 4. Effect of coefficients a_1 and a_2 from equation (7) on the overall oxygen flux at Pe = 10, and hematocrit values of 0.2 and 0.4.

(where both a_1 and a_2 are nonzero). This results in a significant effect of motion on the oxygen transport.

The interpretation of the coefficient a_2 is straight forward. It is the average difference in pO_2 at the plasma-RBC interface of the up- and downstream RBC. In Fig. 4 it is shown that φ is primarily influenced by a_2. The other coefficient, a_1, affects both the curvature of the oxygen profile at the plasma–RBC interfaces and the profile at the plasma–tissue interface. An increase of a_1 results in a steeper profile at the RBC wall and the opposite happens at the tissue wall. The coefficient a_1 hardly influences the oxygen flux through the plasma–tissue interface. This can be interpreted either as insignificant contribution of the curvature of the oxygen profiles or as a cancelation of the effects of the change in curvature of the two profiles.

DISCUSSION

Oxygen transport is based on two phenomena: diffusion and convection. Some of the effects of both of these on oxygen transport can be determined from the local mass transfer rate ratio. Some of the differences in $\dot{m}$ as depicted in Fig. 3 for $R/L = 1.0$ and 0.4 with the boundary conditions of Aroesty and Gross (Figs. 3A and 3C) can be explained by the difference in characteristic time for diffusion ($\tau_D = a^2/D$) and the one for convection ($\tau_v = a/v$), where a is the characteristic distance. The characteristic distance for diffusion to the surrounding tissue is R, which is a constant, and the characteristic distance for convection between two successive RBCs is L. For the data used here $\tau_D/\tau_v = (R/L)^2 \cdot \mathrm{Pe}$, which shows that the characteristic times are equal for Pe = 1.0 and $R/L = 1.0$. The streamlines are independent of the velocity, but they depend on the ratio R/L. For $R/L = 1.0$ the radial velocity component in the plasma is significant at $z = 0.25\ L$, resulting in relatively well-mixed gaps. For low ratios the shape of the streamlines is much flatter and the radial velocity only plays a role close to the RBCs (Bugliarello and Hsiao, 1970). This clarifies the different shapes of $\dot{m}$ for $R/L = 1.0$ and 0.4. In Fig. 3C, the shift to the right of the intersection at $\dot{m} = 1$ near $z = 0$ for higher Pe can be associated with the increase of the ratio τ_D/τ_v. The same arguments hold for Figs. 3B and 3D, but it is much more complicated to understand the implications here, since the boundary concentrations are continuous, nonlinear

functions of r or z. Since the ratio $\dot{m}$ is hard to interpret, the ratio of flux at the capillary border is introduced. Therefore the Figs. 3B and 3D will not be discussed in detail.

The ratio $\varphi(\quad)$ as defined in Eq. (9) depends on the same phenomena as $\dot{m}$, but the contribution of each of these phenomena cannot be determined separately. It does demonstrate, however, the difference in flux at the capillary wall. In Table 1 it is shown that for resting rat heart muscle, an increase in flux of 2 to 7% is calculated depending on the hematocrit. The impact of an increase in flux of, say, 5% is still rather small, since the supplied volume will increase 5% too and therefore the Krogh cylinder radius will only increase with a factor of about $\sqrt{1.05}$, which is an increase of 2%. For maximal flow and a hematocrit of 20% the flux is up to 51% higher than without motion, which would imply a 23% larger radius of the Krogh cylinder. This is a substantial increase. The hematocrit in the capillaries is usually about half the systemic hematocrit, hence the calculations suggest a substantial increase for high flow conditions in rat heart.

Although these results are interesting, no final word can be said about the effect of motion on the oxygen transport. First of all, the influence of the chosen geometry has not been investigated. The geometry used here is applied often in modelling but is certainly not the geometry *in vivo*. Bugliarello and Hsiao (1970) showed that a small flow along the RBCs or a small curvature of the RBCs hardly alters the streamlines. For large deviations of the cylinder geometry, though, or with interaction of RBCs the streamlines are substantially different (Sugihara-Seki, 1992; Sugihara-Seki and Skalak, 1988; Wang and Skalak, 1969) and the oxygen transport is likely to be different, since even without local convection the RBC shape has a large influence on the oxygen concentration profiles (Wang and Popel, 1993). Secondly, the concentrations at the plasma boundaries are assumed to be the same for different Pe numbers. To incorporate changes in boundary concentrations, the model has to be extended to include the binding of oxygen to hemoglobin inside the RBCs and to myoglobin in the tissue and possibly also to convection inside the RBCs. Finally, the values for maximal flow are rough estimates. Values for RBC velocities for maximal working muscle are hard to find in the literature. For resting rat skeletal muscle values of down to 0.1 $mm \cdot s^{-1}$ are reported (Fisher *et al.*, 1992; Tyml *et al.*, 1992). For these values the motion is likely to be insignificant. Tyml (1991) found an average RBC velocity of 0.08 ± 0.07 $mm \cdot s^{-1}$ for resting rat skeletal muscle and a value of 1.0 ± 0.36 $mm \cdot s^{-1}$ for moderately contracting muscle. For contracting muscle the highest value was in the range 2.1–2.2 $mm \cdot s^{-1}$. For maximally working muscle a much higher value for the RBC velocity can be expected than for resting muscle. Even if the maximal flow is half of that assumed here, there still is a notably higher oxygen transfer rate with motion than without motion. It is obvious that it is important to obtain accurate measurements of the upper end of the RBC velocity range, since the effect of motion starts to be important at velocities around 1 $mm \cdot s^{-1}$.

The tissue around the capillary is also a factor of importance. The changes in gradient at the tissue–plasma interface depend on both the gradient in the plasma and the gradient in the tissue. Therefore an accurate model should also calculate the gradient in the tissue adjacent to the capillary. Modelling of an additional thin layer of tissue will suffice, since the gradients damp out quickly (Bos *et al.*, 1995).

CONCLUSION

Aroesty and Gross (1970) stated that the effect of motion is negligible. The outcome of their investigation was determined by their choice of concentrations at the gap boundaries. If the effect of motion were always negligible, then their statement should also be true for boundary concentrations originating from models that neglect the motion. It is shown here that the outcome of their study is often true, but that motion can be a significant factor in oxygen transport when boundary concentrations are used that are similar to those found with the nonmotion models. Although there are some assumptions made in the current model that need further investigation, it is clear that motion of plasma is likely to play a role in the oxygen transfer from the RBCs to the tissue for low hematocrit values and high RBC velocities.

REFERENCES

Altman, P. L., Gibson, J. F., and Wang, C. C. (1958). "Handbook of Respiration" (D. S. Dittmar and R. M. Grebe, Eds.), 403 pp. Saunders, Philadelphia/London.

Aroesty, J., and Gross, J. F. (1970). Convection and diffusion in the microcirculation. *Microvasc. Res.* **2,** 247–267.

Bird, R. B., Stewart, W. E., and Lightfoot, E. N. (1960). "Transport Phenomena," 780 pp. Wiley, New York.

Bos, C., Hoofd, L., and Oostendorp, T. (1995). Mathematical model of erythrocytes as point-like sources, *Math. Biosc.* **125,** 165–189.

Bugliarello, G., and Hsiao, G. C. (1970). A mathematical model of the flow in axial plasmatic gaps of the smaller vessels. *Biorheology* **7,** 5–36.

Duda, J. L., and Vrentas, J. S. (1971). Steady flow in the region of closed streamlines in a cylindrical cavity. *J. Fluid Mech.* **45,** 247–260.

Fisher, A. J., Schrader, N. W., and Klitzman, B. (1992). Effects of chronic hypoxia on capillary flow and hematocrit in rat skeletal muscle. *Am. J. Physiol.* **262,** H1877–H1883.

Groebe, K., and Thews, G. (1989). Effects of red cell spacing and red cell movement upon oxygen release under conditions of maximally working skeletal muscle. *In* "Oxygen transport to tissue XI." *Adv. Exp. Med. Biol.* **248,** 175–185.

Groebe, K. (1990). A versatile model of steady state O_2 supply to tissue. Application to skeletal muscle. *Biophys. J.* **57,** 485–498.

Gross, J. F., and Aroesty, J. (1972). Mathematical models of capillary flow: A critical review, *Biorheology* **9,** 225–264.

Honig, C. R. (1981). "Modern cardiovascular physiology." 347 pp. Little, Brown and Co., Boston.

Hoofd, L., Olders, J., and Turek, Z. (1990). Oxygen pressures calculated in a tissue volume with parallel capillaries. *In* "Oxygen transport to tissue XII." *Adv. Exp. Med. Biol.* **277,** 21–29.

Hoofd, L. (1992). Updating the Krogh model—Assumptions and extensions. *In* "Oxygen transport in biological systems," Society for Experimental Biology Seminar Series 51, (S. Eggington and H. F. Ross, Eds.), pp. 197–229. Cambridge Univ. Press, Cambridge.

Huang, H. K. (1971). Theoretical analysis of flow patterns in single-file capillaries. *J. Biomech.* **4,** 103–112.

Krogh, A. (1919). The number and distribution of capillaries in muscles with calculations of the oxygen pressure head necessary for supplying the tissue. *J. Physiol.* **52,** 409–415.

Leonard, E. F., and Jørgensen, S. B. (1974). The analysis of convection and diffusion in capillary beds. *Annu. Rev. Biophys. Bioeng.* **3,** 293–339.

Lew, H. S., and Fung, Y. C. (1969). The motion of the plasma between the red cells in the bolus flow. *Biorheology* **6,** 109–119.

Lochner, W. (1971). Herz, *In* "Physiologie des Kreislaufs I." (E. Bauereisen, Ed.), pp. 185–228. Springer-Verlag, Berlin/Heidelberg/New York.

Nair, P. K., Huang, N. S., Hellums, J. D., and Olson, J. S. (1990). A simple model for prediction of oxygen transport rates by flowing blood in large capillaries. *Microvasc. Res.* **39,** 203–211.

Prothero, J., and Burton, A. C. (1961). The physics of blood flow in capillaries. I. The nature of the motion. *Biophys. J.* **1,** 565–579.

Rakusan, K., and Blahitka, J. (1974). Cardiac output distribution in rats measured by injection of radioactive microspheres via cardiac puncture. *Can. J. Physiol. Pharmacol.* **52,** 230–235.

Secomb, T. W., Hsu, R., Dewhirst, D. V. M., Klitzman, B., and Gross, J. F. (1993). Analysis of oxygen transport to tumor tissue by microvascular networks. *Int. J. Radiat. Oncol. Biol. Phys.* **25,** 481–489.

Sharan, M., Singh, B., Singh, M. P., and Kumar, P. (1991). Finite element analysis of oxygen transport in the systemic capillaries. *IMA J. Math. Appl. Med. Biol.* **8,** 107–123.

Sugihara-Seki, M. (1992). Motion of a doublet of two cylinders in contact in a narrow channel flow. *J. Biomech. Eng.* **114,** 546–549.

Sugihara-Seki, M., and Skalak, R. (1988). Numerical study of asymmetric flows of red blood cells in capillaries. *Microvasc. Res.* **36,** 64–74.

Tsai, A. G., and Intaglietta, M. (1993). Evidence of flowmotion induced changes in local tissue oxygenation. *Int. J. Microcirc. Clin. Exp.* **12,** 75–88.

Tyml, K. (1991). Heterogeneity of microvascular flow in rat skeletal muscle is reduced by contraction and by hemodilution. *Int. J. Microcirc. Clin. Exp.* **10,** 75–86.

Tyml, K., Mathieu-Costello, O., and Budreau, C. H. (1992). Distribution of red blood cell velocity in capillary network, and endothelial ultrastructure, in aged rat skeletal muscle. *Microvasc. Res.* **44,** 1–13.

Van Citters, R. L., and Franklin, D. L. (1969). Cardiovascular performance of Alaska sled dogs during exercise. *Circ. Res.* **24,** 33–42.

Wang, C.-H., and Popel, A. S. (1993). Effect of red blood cell shape on oxygen transport in capillaries. *Math. Biosci.* **116,** 89–110.

Wang, H., and Skalak, R. (1969). Viscous flow in a cylindrical tube containing a line of spherical particles. *J. Fluid Mech.* **38,** 75–96.